IGNITABILITY LIMITS FOR COMBUSTION OF UNINTENDED HYDROGEN RELEASES: EXPERIMENTAL AND THEORETICAL RESULTS

Schefer, R.W.[1], Evans, G.H.[1], Zhang, J.[1], Ruggles, A.J.[1], and Greif, R.[2]
[1] Combustion Research Facility, Sandia National Laboratories, Livermore, CA, 94551, USA, rwsche@sandia.gov
[2]Mechanical Engineering Department, University of California, Berkeley, CA, 94720, USA, greif@me.berkeley.edu

ABSTRACT

The ignition limits of hydrogen/air mixtures in turbulent jets are necessary to establish safety distances based on ignitable hydrogen location for safety codes and standards development. Studies in turbulent natural gas jets have shown that the mean fuel concentration is insufficient to determine the flammable boundaries of the jet. Instead, integration of probability density functions (PDFs) of local fuel concentration within the quiescent flammability limits, termed the flammability factor (FF), was shown to provide a better representation of ignition probability (P_I). Recent studies in turbulent hydrogen jets showed that the envelope of ignitable gas composition (based on the mean hydrogen concentration), did not correspond to the known flammability limits for quiescent hydrogen/air mixtures. The objective of this investigation is to validate the FF approach to the prediction of ignition in hydrogen leak scenarios. The P_I within a turbulent hydrogen jet was determined using a pulsed Nd:YAG laser as the ignition source. Laser Rayleigh scattering was used to characterize the fuel concentration throughout the jet. Measurements in methane and hydrogen jets exhibit similar trends in the ignition contour, which broadens radially until an axial location is reached after which the contour moves inward to the centerline. Measurements of the mean and fluctuating hydrogen concentration are used to characterize the local composition statistics conditional on whether the laser spark results in a local ignition event or complete light-up of a stable jet flame. The FF is obtained through direct integration of local PDFs. A model was developed to predict the FF using a presumed PDF with parameters obtained from experimental data and computer simulations. Intermittency effects that are important in the shear layer are incorporated in a composite PDF. By comparing the computed FF with the measured P_I we have validated the flammability factor approach for application to ignition of hydrogen jets.

1.0 INTRODUCTION

One of the primary hazards associated with unintended H_2 releases is the consequence of ignition of the resulting H_2/air mixture which can occur over a much wider range of composition compared with typical hydrocarbon/air mixtures (e.g., lower and upper static flammability limits (LFL and UFL) of 0.04 and 0.75 mole fraction, respectively, of H_2 in air compared with 0.053 and 0.15 for natural gas). Previous experimental studies [1,2] have shown that the ignitable gas composition envelope (based on mean values) in turbulent H_2 leaks does not correspond well to the known flammability limits for static H_2 mixtures. Studies using pulsed ignition sources on turbulent natural gas jets [3-5] have shown that the flammable boundary of the jet extends farther radially from the jet exit and is shortened axially when compared to the static LFL boundary because turbulent transport is not accounted for in determining the static flammability limits. It was found that direct integration of probability distribution functions (PDFs) of the fuel concentration between the flammability limits to form the flammability factor (FF) gives the true probability of ignition (P_I). Knowledge of the ignition limits resulting in sustained combustion of H_2 under conditions relevant to unintended releases is essential for codes and standards development which relies on probabilistic risk assessment of accident scenarios, the consequences of which must be determined using ignition limits.

There are two primary objectives of the present study. The first objective which is of particular interest to safety codes and standards development is to experimentally characterize and quantify the H_2/air

flammability limits that define ignitability as a function of the flow conditions typically found in H_2 releases. In addition, several research groups have developed models to predict P_I in turbulent jet flows of conventional hydrocarbon fuels (primarily CH_4) and have shown varying degrees of success. Thus a second objective of the present work is to utilize and validate a theoretical approach for predicting ignition in H_2 leak scenarios using the data base obtained in these experiments.

2.0 EXPERIMENTAL

The flow apparatus consisted of a 1.91-mm diameter vertical jet tube through which the H_2 was injected. The tube was located in the center of a co-flow air stream. To reduce flow non-uniformity and the influence of room air disturbances the air exited through a 30 x 30 cm honeycomb section with a velocity of 0.3 m/s. This co-flow air velocity is sufficiently low to have a negligible influence on the central jet flow [6]. A CH_4 jet was also used to provide comparisons with the H_2 jet under conditions of identical geometry and to compare with previously published results. The flow rates of both fuels were metered using calibrated mass flow controllers (MKS) to estimated accuracies of better than 1 percent. Jet exit velocities of 134 m/s for H_2 and 29 m/s for CH_4 gave Reynolds and Froude numbers (based on the jet exit diameter) of 2384 and 268, respectively, for H_2 and 3406 and 238 for CH_4. Previous experiments without co-flow [7,8] showed that the H_2 jet at this Froude number and over the range of downstream distances considered is momentum-dominated with small effects of buoyancy.

The experimental system shown in Fig. 1 was developed to study the ignition characteristics of H_2 in turbulent flows using a non-intrusive laser ignition source. Previous studies [5,9] in CH_4 flames used a spark ignition system which has the disadvantage that the electrodes inserted in the flow can affect the measurements. The 532 nm Nd:YAG laser beam, with a pulse energy and duration of up to 1 Joule and 9-nsec, respectively, is focused using suitable optics to a 0.2 mm diameter spot, providing 100 mJ of laser power, sufficient to cause a spark and ignite a flammable H_2/air mixture. Thermocouples mounted downstream of the ignition location were used to determine whether a local ignition event in the form of a flame kernel that was subsequently extinguished occurred (indicated by a short-duration spike in the gas temperature originating from the ignition point), or whether ignition resulted in complete light-up of the jet (indicated by a rapid rise in gas temperature to a constant high temperature value). The experiment was automated with a software program based on Labview.

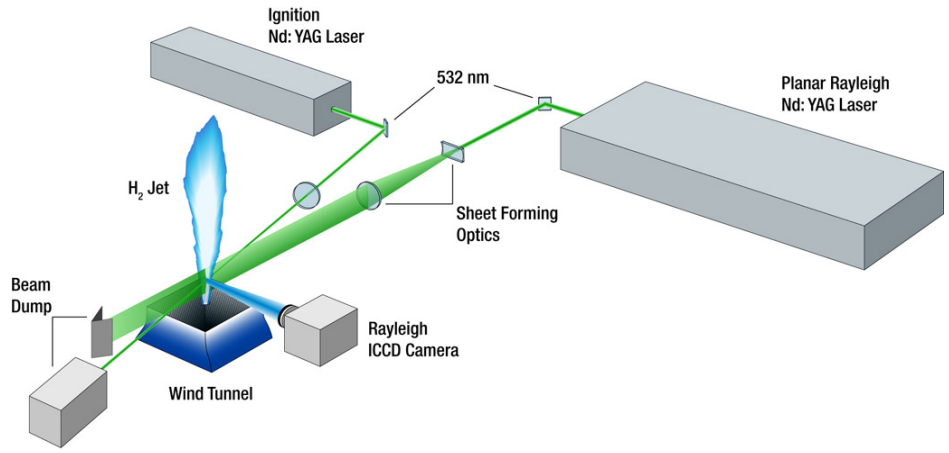

Figure 1. Laser ignition system and Rayleigh-scattering system for turbulent jet ignition study.

Planar Laser Rayleigh Scattering (PLRS) imaging was used to measure the H_2 and CH_4 concentration distributions. Details can be found in [7,8]. The laser light was provided by a second Nd:YAG laser (9-ns pulse duration, 800 mJ/pulse) operating at a wavelength of 532 nm. The beam was formed into a 75-mm high and 0.3-mm thick sheet of light by a 50-mm focal length cylindrical lens followed by a 500-mm focal length spherical lens combination. The Rayleigh-scattering signal was collected at right

angles to the laser sheet (f/1.2 optics) and focused onto an intensified Roper Scientific PI-MAX ICCD camera. The camera intensifier was gated to stay on for 400 nsec to reduce flame luminescence and background-scattered light. For the vertically-oriented jet, the plane of the laser sheet was parallel to the jet centerline. The imaged field-of-view for the camera was approximately 50 mm (radial direction) x 50 mm (axial direction). The camera detector was operated in a 512 x 512 pixel format, which provided a spatial resolution of about 100 µm per pixel. The PLRS imaging technique was used to measure the time-averaged flow properties and the instantaneous concentration distribution in the local region of an ignition event. Since the PLRS imaging measurement is done nearly simultaneously with the laser ignition (actually it precedes the laser ignition by 320 msec), the local composition in the area of the ignition point can be determined conditional on whether there is a local ignition and a complete subsequent light-up or whether the ignition kernel is subsequently extinguished.

3.0 EXPERIMENTAL RESULTS

Shown in Fig. 2 are the time-averaged (mean, Fig. 2a) and fluctuating (rms, Fig. 2b) H_2 mole fraction (X_{H2}) distributions for the H_2 jet (color bars to the right of the images show magnitude) where the axial (z) and radial (y) coordinates are normalized by the jet exit diameter, d. These images are averaged over 400 single-shot images. The jet exit is located at the bottom center of the images and the jet is directed vertically upward. The highest H_2 concentrations are found near the jet exit before significant mixing with ambient air occurs. Farther downstream the H_2 concentration decreases rapidly as air is entrained into the high velocity central jet. The axial decay rate of X_{H2} follows a 1/z dependence. The maximum fluctuations are found in the shear layer between the central jet and the ambient air where the gradient in X_{H2} is highest. Fig. 2c is an image from a single laser shot. Due the short 8-nsec duration of the laser pulse, this image reveals the instantaneous structure of the H_2 concentration field. In contrast to the smooth distributions of Figs. 2a,b, random spatial variations are readily apparent in the H_2 concentration in Fig. 2c. These variations are caused by the interaction of the turbulent jet flow of H_2 mixing with ambient air, resulting in a spatially- and temporally-varying H_2 distribution. The corresponding images for the CH_4 jet (not shown) are similar to the H_2 jet; the time-averaged (mean) CH_4 mole fraction decreases along the centerline with downstream distance and the maximum concentration fluctuations occur in the jet shear layer. The single-shot, instantaneous images reveal a complex distribution in CH_4 concentration, similar to that shown for H_2.

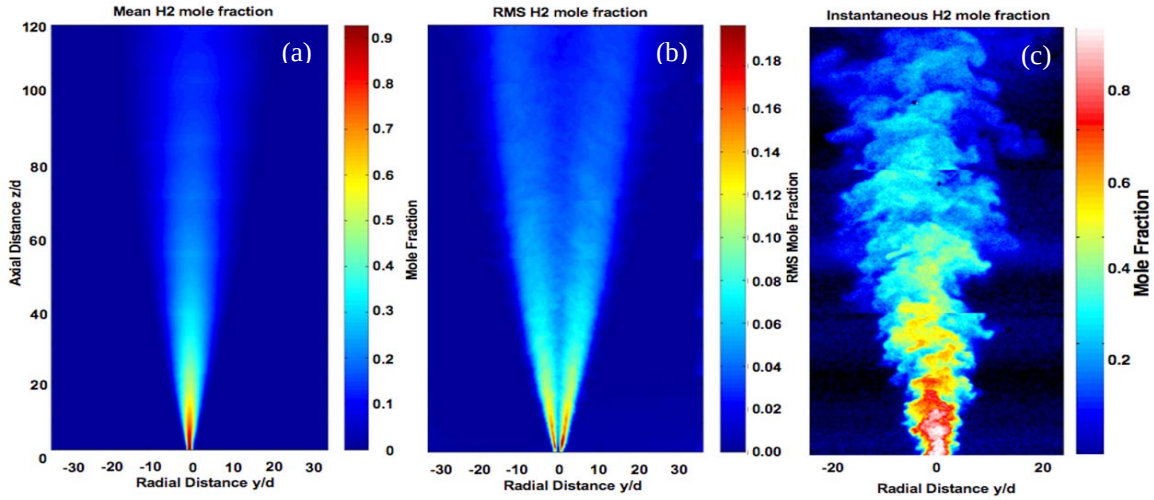

Figure 2. Time-average images obtained in hydrogen jet at u_j=134 m/s, Re=2,384. (a) mean hydrogen mole fraction; (b) rms fluctuations of hydrogen mole fraction; (c) instantaneous image.

In [5] it was determined that a successful local ignition event in a natural gas jet depends primarily on the location of the spark. In some regions of the flow, the spark resulted in ignition each time a spark

was applied, while in other regions successful ignition events were not observed. A critical surface called the light-up boundary was identified within the jet that separates the ignition characteristics of the flow into two regions: (1) nearest the central part of the jet at moderate downstream distances, the flame kernel resulting from local ignition propagates outward from the ignition point giving rise to the complete light-up of the jet and the formation of a continuous, stable flame; (2) radially outward toward the ambient air, the flame kernel and any flame generated is convected downstream where it is eventually extinguished. The probability of whether an ignition event and flame kernel is initially formed by the spark, termed P_I (the number of ignition successes divided by the number of ignition trials), and the probability of whether a spark leads to complete flame light-up (stable flame), termed P_L, were also quantified in [9] along the centerline of natural gas and propane jets.

To determine the jet light-up boundary, the spark system was run at 10 Hz and the burner was slowly translated in the radial direction, moving closer to the spark until complete light-up of the jet was observed. The measured jet light-up contours for the H_2 and CH_4 jets are shown in Fig. 3. Both jets exhibit similar trends, with the light-up contours moving outward radially with downstream distance until a point is reached where the contours move inward toward the jet centerline. At all axial locations, the H_2 contour is always located at a greater radial distance than CH_4. The outward spread of the CH_4 contour agrees well with that found in [5].

The mean H_2 concentration contours of 8%, 0.5%, and 4% are also shown in Fig. 3a (note 4% is the LFL of a static mixture of H_2 and air). The 5.3% concentration contour of CH_4 (corresponding to the LFL of CH_4) is shown in Fig. 3b. For both H_2 and CH_4 the light-up boundary extends radially into time-averaged mixtures considerably leaner than the LFL, more closely following the 0.005 mole fraction contour with both fuels. Clearly, if the complete light-up of a turbulent fuel jet can occur at a mean concentration that is only 10% of the LFL, this would have significant implications for safety distances in various accident scenarios.

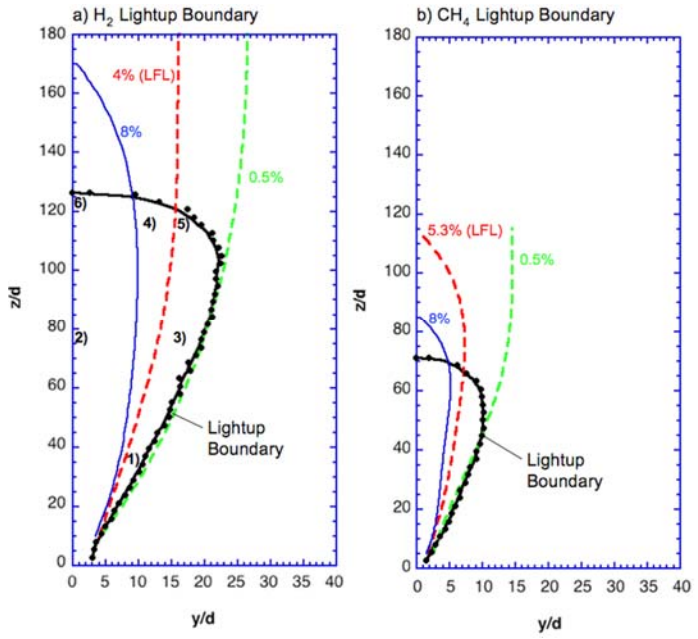

Figure 3. Jet light-up contours for the H_2 and CH_4 test cases. Each point is the mean of five tests.

The maximum axial distance at which flame light-up can occur is considerably shorter than the axial distance to the LFL concentration contour. The light-up probability, P_L, along the centerline of the H_2 jet and the corresponding variation in $1/X_{H2}$ are presented in Fig. 4a. For $10<z/d<100$, P_L is equal to unity since an ignition event always leads to flame light-up. Limited measurements (not shown) obtained near the jet exit also show that at distances sufficiently close to the jet exit ($z/d < 10$) no

flame light-up could be obtained (X_{H2}>UFL). For z/d >140, P_L=0 and all ignition events are extinguished. Comparison with $1/X_{H2}$ in Fig. 4a shows that no flame light-up can be achieved along the centerline for $X_{H2} \leq 0.08$ to 0.10. This concentration range is considerably higher than the LFL of 0.04 , but is in good agreement with the measurements of [2], who found that stable flame ignition could not be achieved near the centerline for $X_{H2} \leq 0.08$. The centerline variation in P_I in Fig. 4a shows that a finite probability for local ignition exists for z/d<350. Comparison with $1/X_{H2}$ shows that P_I falls to zero when $X_{H2} \approx$LFL. For z/d<120, both P_I and P_L are unity, indicating each laser spark always results in jet light-up. In contrast, for 140<z/d<350 there is a finite probability that a laser spark will result in a flame kernel, but the kernel is always extinguished. For z/d>350, local ignition is never observed. The corresponding centerline profiles for the CH_4 jet are shown in Fig. 4b. Immediately downstream of the jet exit no ignition is observed since insufficient mixing with air has occurred; P_I then increases to unity before decreasing again to zero for z/d>120. As seen with H_2, P_I falls to zero where the concentration is slightly leaner than the LFL, or about 0.8LFL. Further comparison with the H_2 jet in Fig 4a shows that the range of centerline distances over which a high P_I exists in the CH_4 jet, 10 < z/d<130, is considerably narrower than in the H_2 jet where ignition events are observed between 5< z/d<350. For example, for H_2 a P_I value of unity is measured at z/d>5, while in the CH_4 jet it does not reach unity until z/d>70. The likely reason for this behavior is due to the wider flammability limits of H_2.

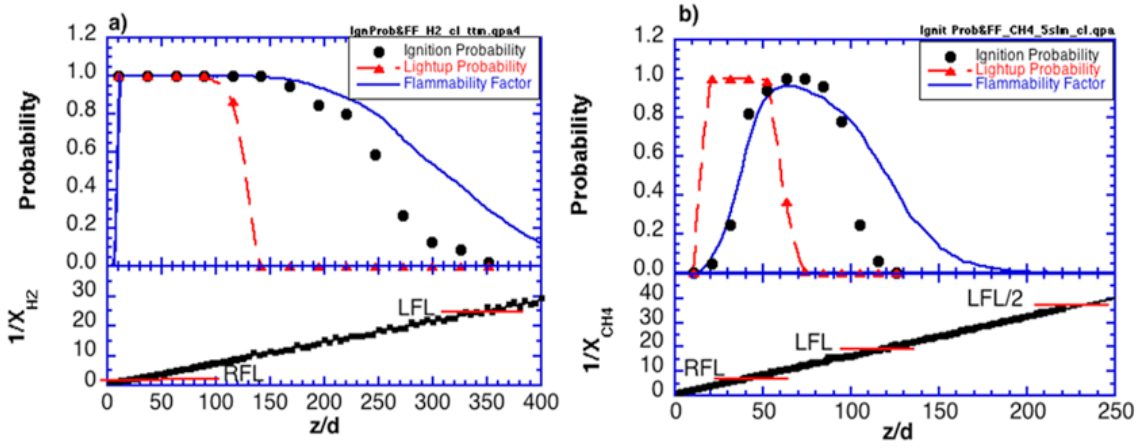

Figure 4. Centerline profiles of ignition and light-up probability and flammability factor. Lower graphs show inverse centerline mole fraction. (a) H_2 jet; (b) CH_4 jet.

Radial profiles of P_I and P_L for the H_2 jet are shown in Fig. 5 at four axial (z) locations. In the central part of the jet both P_I and P_L equal one and decrease to zero at large r/d where the fuel is diluted. One exception to this is at z=220 mm where the light-up probability reaches a maximum of only 0.88 even in the central jet. This can be attributed to the increasingly lean fuel/air mixtures which can no longer support the initiation of combustion at large z. In general, the width of the region where P_I>0 increases with downstream distance.

It was shown in Fig. 3 that light-up is observed at radial locations where the mean fuel concentration is considerably smaller than the LFLs of both H_2 and CH_4 jets. This result is consistent with the concept of intermittency in turbulent jets of fuel into either quiescent [5] or a cross-flow [10] of air where, at a fixed point, the turbulent interface between the jet and air is highly irregular (cf. Fig. 2c) and varies with time. This situation results in bimodal PDFs, with a single spike at zero fuel concentration corresponding to pure air and a broader distribution over a range of fuel concentrations corresponding to mixtures of fuel and air. Although the mean concentration can be quite low (i.e. below the LFL of the fuel) with a significant probability of pure air, there is still a finite probability that a flammable mixture will exist at large r/d. Clearly, time-averaged LFLs established in uniformly-mixed, quiescent

experimental systems do not correspond well with the region over which a stable flame is produced, or light-up is observed, in turbulent jet flows. It was concluded in [4,9] that conventional flammability limits have little value in establishing the flammable boundaries of turbulent hydrocarbon jet flows. The present study confirms the extension of these findings to turbulent H_2 flows.

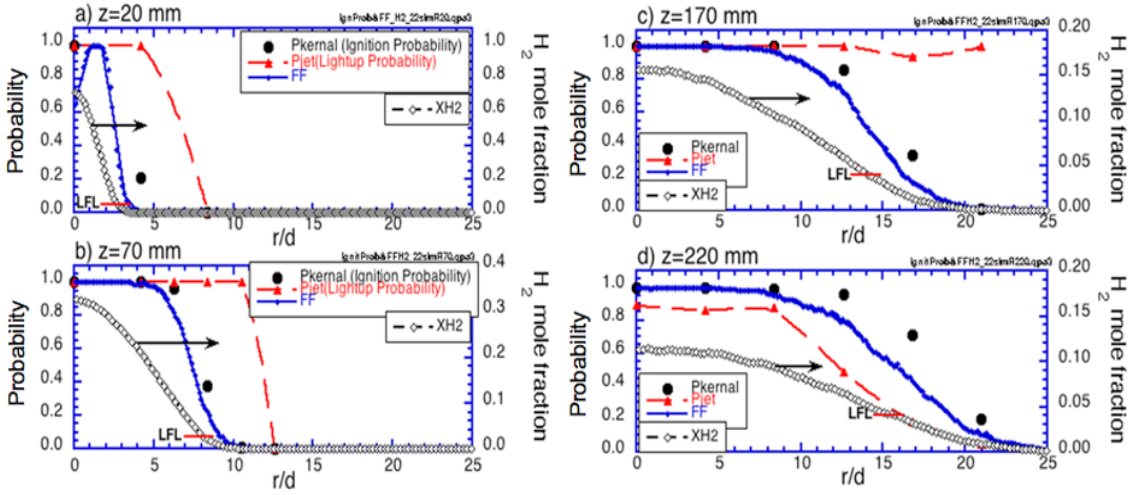

Figure 5. Radial profiles of ignition and light-up probability, flammability factor and H_2 mole fraction in the hydrogen jet. a) z=20 mm; b) z=70 mm; c) z=170 mm; d) z=220 mm.

The flammability factor, FF, which is the cumulative probability of finding a flammable mixture at a given point in a turbulent flow, is discussed in the section Modeling Ignition Probability. The FF, determined experimentally from the total data set of up to 400 images as the fraction of time that the H_2 concentration falls within the flammability limits, is shown in Fig. 4a. Both FF and P_I equal one for z/d<170, beyond which P_I falls more rapidly to zero. In Fig. 4b for the CH_4 jet, FF shows excellent agreement with P_I for z/d<90; for larger z/d P_I falls more rapidly to zero. This result is surprising since excellent agreement between P_I and FF was found in [5] at all locations along the centerline of a natural gas jet. Comparisons between FF and P_I for the H_2 jet in the radial direction are shown in Fig. 5 where there is reasonable agreement at all locations. Similar agreement between radial profiles of FF and P_I was found for the CH_4 jet (not shown). It is concluded that the FF provides a good measure of P_I in turbulent H_2 jet flows.

PLRS was used to quantify the fuel concentration at the point where the laser spark initiates a flame kernel in order to characterize conditions leading to ignition. At each location up to 100 PLRS images were obtained prior to firing the laser pulse and the outcome of the laser ignition pulse (i.e., no ignition or ignition leading to either complete flame light-up or subsequent extinction) was also recorded. Two probability distributions, $P(X_{H2})$, are shown in Fig. 6 at location labeled 1) in Fig. 3a which is within the shear layer at z/d=36. The distribution of Fig. 6a, obtained from 400 images taken at random times with no laser ignition pulse, shows a nonzero probability at X_{H2}=0 and zero probability for X_{H2}>0.15. The probability distribution conditional on the light-up of a stable flame is shown in Fig. 6b to extend from X_{H2}=0.15, which is the maximum concentration seen in the unconditioned distribution, to a minimum concentration of X_{H2}=0.04. Light-up does not occur for X_{H2}<LFL even though the unconditioned distribution at this location shows that mixtures with X_{H2}<LFL do exist. Thus, while the time-averaged concentration distribution at a location is not sufficient to determine whether ignition occurs, ignition does require X_{H2} to be greater than LFL at the time and location of the laser ignition spark. Distributions at other locations confirm that if the local composition at the time of the laser spark is less than the LFL of X_{H2}=0.04, neither ignition nor subsequent light-up occurs.

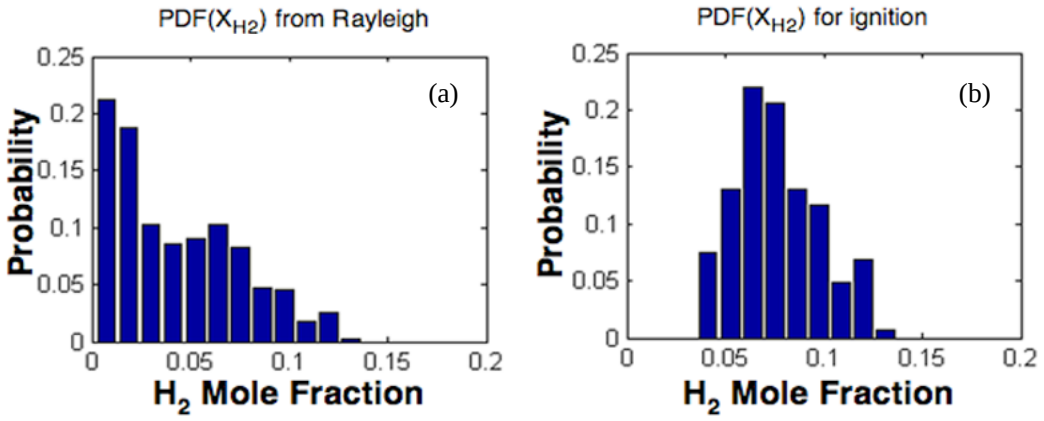

Figure 6. Probability distributions, $P(X_{H2})$, of X_{H2} at z/d=36.6, r/d=8.4; (a) unconditional (no laser pulse); (b) conditional.

4.0 MODELING IGNITION PROBABILITY

4.1 Probability Density Function (PDF) and Intermittency

Probability density function (PDF) methods are related to the likelihood (probability) that the concentration of fuel has values between certain limits [11]. A Gaussian PDF that depends on the average and the rms values of the concentration of the fuel was shown to be a good choice for turbulent jets of natural gas, propane, and a gas with a large content of H_2 [9]:

$$\mathcal{P}_{\mathrm{G}}(c) \equiv \frac{1}{\sqrt{2\pi}c_{\mathrm{rms}}} \exp\left\{-\left(c-\bar{c}\right)^2 \Big/ \left(2c_{\mathrm{rms}}^2\right)\right\} \tag{1}$$

where c represents mole, mass, or mixture fraction of fuel. Integrating the PDF from the LFL to the UFL defines the flammability factor (FF) in [5]:

$$\mathrm{FF} \equiv \int_{c_{\mathrm{LFL}}}^{c_{\mathrm{UFL}}} \mathcal{P}(c)dc \quad . \tag{2}$$

For a Gaussian PDF

$$\mathrm{FF}_{\mathrm{G}} = \frac{1}{2}\left[\mathrm{erf}\left(\frac{c_{\mathrm{UFL}}-\bar{c}}{\sqrt{2}c_{\mathrm{rms}}}\right) - \mathrm{erf}\left(\frac{c_{\mathrm{LFL}}-\bar{c}}{\sqrt{2}c_{\mathrm{rms}}}\right)\right] \quad . \tag{3}$$

Good agreement between FF (with experimentally measured mean and variance of fuel concentration) and P_I was obtained along the centerline of jets of CH_4, C_3H_8, and town gas in [9]. However, due to the bimodal nature of turbulent mixing of fuel and air, the PDF is not represented well by a normal distribution off the jet centerline especially in the shear layer where there is a large probability of air without fuel being present. As noted in [12,13] an important characteristic of turbulent jets is the concept of intermittency, quantified in the intermittency factor γ, defined to be the fraction of time at a point in the flow that the mixture fraction f is greater than a small threshold value [14]. Note that γ ranges from 0 in the non-turbulent air outside the shear layer to 1 along the centerline of the turbulent jet flow. For a turbulent jet of unignited H_2 into air, f is equal to the mass fraction of H_2. It was noted in [15] that the PDF in the intermittent region of heated jets and wakes could be described in terms of a composite PDF in which a Gaussian (normal) PDF, used to describe the turbulent fluid and weighted with γ, was combined with a delta function, used to describe the non-turbulent fluid:

$$\mathcal{P}_c(f) \equiv (1-\gamma)\delta(f) + \gamma \mathcal{P}_G(f) \quad . \tag{4}$$

This composite PDF gave good agreement in [5] between FF and the measured P_I of CH_4 along a radial line 40 jet diameters downstream of the exit. Data from several turbulent shear flows was used in [16] to show that γ could be approximated by a linear relationship with the square of the concentration intensity:

$$\gamma \cong \frac{K+1}{\overline{f''^2}/\overline{f}^2 + 1} \tag{5}$$

where $K \cong 0.25$; more recently in [17] the intermittency was determined by solving a transport equation for γ. In evaluating PDFs and FFs the required parameters $\overline{f}$, $\overline{f''^2}$, and γ have been obtained from both experimental data and model results. For example, a *k*-ε-γ turbulence model was used recently [18] along with a presumed three-part PDF to predict the P_I both along and off the centerline of several turbulent fuel jets. In addition to the fluid conservation and turbulence model equations, transport equations for the mixture fraction *f*, variance of the mixture fraction $\overline{f''^2}$, and intermittency factor γ, were solved. The predicted PDFs and FFs were in fair agreement with experimentally determined quantities both along the centerline of the jets and at radial locations away from the centerline. We note the work in [19] in respect to composite PDFs.

4.2 Results

In this section we present model predictions of the flammability factor (FF) for two probability density functions (PDFs), the Gaussian PDF of equation (1) with FF given in equation (3) (with *c* in those equations replaced by *f*), and a two part composite PDF:

$$\mathcal{P}_c(f) \equiv (1-\gamma)\delta(\varepsilon)\left[H(f) - H(f-\varepsilon)\right] + \gamma \mathcal{P}_G(f)\left[H(f) - H(f-1)\right] \tag{6}$$

where $H(x)$ is the Heaviside step function, $H(x) = 0$ for $x < 0$; $H(x) = 1$ for $x \geq 0$; ε is a small number (0.0025), and δ is defined such that

$$\int_0^1 \mathcal{P}_c(f)\, df = 1 \tag{7}$$

with FF given by

$$\mathrm{FF}_c = \gamma \int_{f_{\mathrm{LFL}}}^{f_{\mathrm{UFL}}} \mathcal{P}_G(f)\, df = \gamma \mathrm{FF}_G \tag{8}$$

and where the intermittency factor γ is given by (5). The parameters (mean and rms of fuel concentration) required for evaluation of the PDFs that are integrated to determine the FFs are obtained from either experimental data or model predictions. Predicted and measured PDFs for the H_2 jet are compared at two locations, one far off the jet centerline where intermittency is significant ($\gamma < 1$) and one closer to the jet centerline where $\gamma \approx 1$. Predicted and measured FFs are compared with measured P_I; comparisons are shown for both axial profiles along the jet centerline and radial profiles at various axial locations downstream of the jet exit.

Because results will be presented in which the predicted FF depends on parameters obtained from CFD modeling of turbulent jets, it is important to validate the determination of those quantities, independent of the assumed PDF. The CFD code Fuego [20] has been used to model turbulent

isothermal jets of fuel into air and calculate f and $\overline{f''^2}$. The calculated decay rates of the centerline concentration of turbulent fuel jets into ambient air have been validated by comparing with several experimental data sets; good agreement was obtained for H_2 and CH_4 (not shown). The centerline variations of the predicted rms of the mixture fraction fluctuations $\sqrt{\overline{f''^2}}$ were also validated by comparing with measured values for the same jets (not shown). Again good agreement is obtained except for the peak values which occur within 10 jet diameters downstream of the jet exit. Close to the jet exit there are large uncertainties in the measured rms values; in addition the predicted values near the jet exit are sensitive to jet exit boundary conditions.

To validate the composite PDF given in (6), comparisons between predicted and measured PDFs are shown at two locations in the H_2 jet in Fig. 7. The bimodal nature of the PDF at r/d=7.85; z/d=50 is predicted by the composite PDF using model parameters (with γ=0.87 at this location, from equation (5)) in Fig. 7a and agrees well with the measured PDF. The Gaussian PDF predicted using model parameters is also shown in Fig. 7a for reference; it does not capture the large increase in the PDF that occurs at small values of f caused by the intermittency of the turbulent shear layer. Predicted and measured PDFs closer to the jet centerline are shown in Fig. 7b at r/d=2.1; z/d=50. At this location, equation (5) gives $\gamma \approx 1$ and there is no difference between the composite and Gaussian (not shown) PDFs. The predicted PDF is shifted toward larger f and the peak value is smaller compared with the measured PDF in Fig. 7b. It is noted that the measured PDFs were determined in terms of X_{H2}; for comparison to the predicted PDFs in terms of f the measured X_{H2} was converted to mass fraction and the measured PDFs were scaled so that integrals over mass (mixture) fraction were equal to 1.

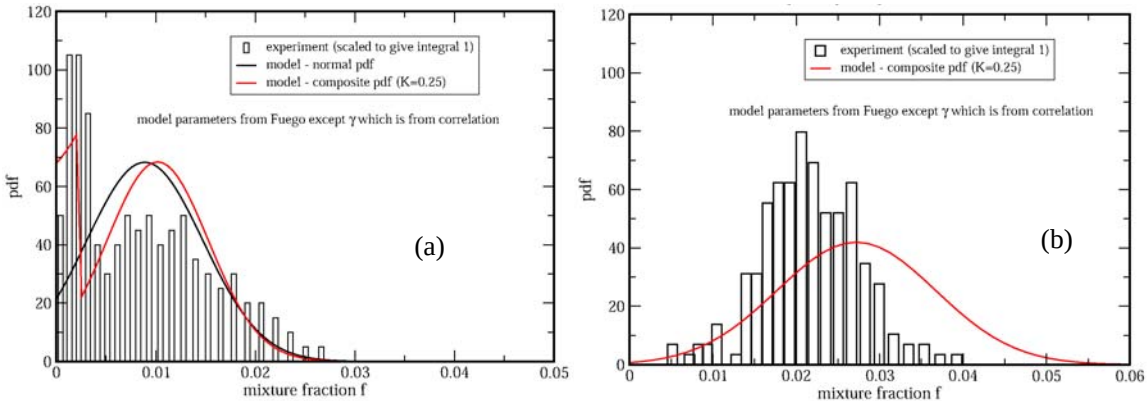

Figure 7. Predicted and measured PDfs in the unignited vertical free jet of H_2 into air (Re=2384; Fr=268; d=1.91 mm) at z/d =50; (a) r/d =7.85; (b) r/d = 2.1.

Predicted and measured FFs and measured P_Is along the centerlines of H_2 and CH_4 jets are shown in Figs. 8a and 8b, respectively. Predicted FFs are determined for both Gaussian and two part composite PDFs in Fig. 8 where the Gaussian PDF parameters are evaluated from both experimental data and model results and the composite PDF parameters are evaluated using model results with K=0.25 in (5). For the H_2 jet in Fig. 8a, the predicted FF using a Gaussian PDF evaluated with experimental parameters (black curve) is in good agreement with the measured FF (solid red curve) for z/d<260; for z/d>260 the predicted FF is larger than the measured FF. For the CH_4 jet in Fig. 8b, the corresponding curves are in excellent agreement throughout the flammable range of the jet. When the Gaussian PDF is evaluated using model parameters, the predicted FF for the H_2 jet (green curve) is in slightly better agreement with the measured FF for z/d>260; for the CH_4 jet in Fig. 8b, however, the Gaussian PDF evaluated with model parameters (green curve) yields a predicted FF that is smaller than the measured FF. This may be related to the smaller predicted than measured average values of CH_4 mole fraction along the centerline of the jet for z/d>75 (not shown). For both H_2 and CH_4 jets, there is no difference in the predicted FF using either the composite PDF or the Gaussian PDF. This is to be expected since

γ =1 along the centerlines of the jets. For the H_2 jet in Fig. 8a, the predicted FF agrees well with the measured P_I for z/d<180, beyond which P_I drops more rapidly than either predicted or measured FF. A similar trend occurs for the CH_4 jet in Fig. 8b where the measured PI falls below the measured or predicted FF for z/d>100. This discrepancy was not seen for the natural gas jet studied in [5]. The experimental determination of P_I at locations far downstream of the jet exit where the fuel concentration is small may have a large uncertainty; ignition events where a flame kernel is formed and then quickly extinguished may not be detected in the experiment. Also shown in Figs. 8a,b are the experimental average mole fractions of H_2 and CH_4 along the centerlines of the jets and the static LFL and UFL values (0.04 and 0.75, respectively, for H_2; 0.05 and 0.15, respectively, for CH_4).

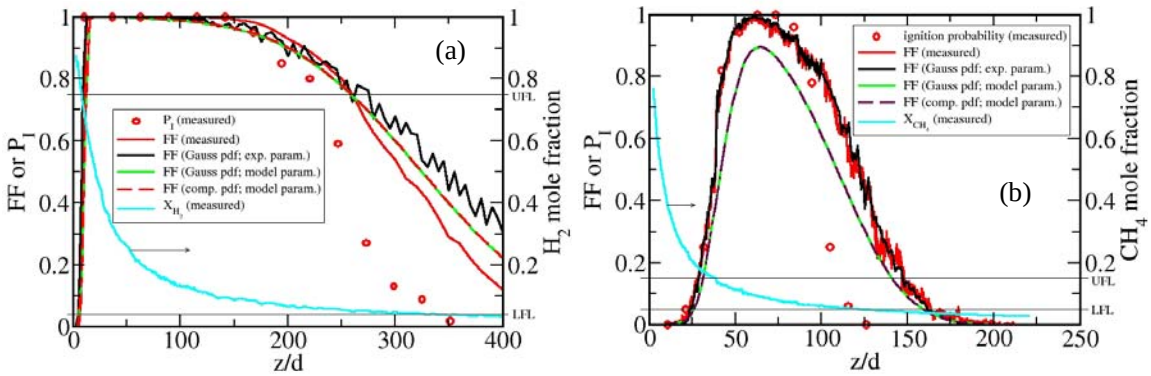

Figure 8. Predicted and measured FFs, measured P_Is, and measured average mole fractions of fuel along the centerlines of vertical free jets of fuel into air: (a) H_2 (Re=2384; Fr=268); (b) CH_4 (Re=3406; Fr=238); d =1.91 mm; also shown are LFL and UFL values.

Predicted and measured FFs and measured P_Is along radial lines at two axial locations downstream of the jet exit are shown in Fig. 9 for H_2. Predicted FFs are determined for both Gaussian and two-part composite PDFs in Fig. 9 where the PDF parameters are evaluated using model results. At z/d=89 shown in Fig. 9a, the predicted FFs using the Gaussian PDF (green curve) and the composite PDF (orange curve) are in good agreement with the measured FF (solid red curve) and with the measured P_I. At z/d=220 shown in Fig. 9b, the predicted FFs agree qualitatively with the measured P_I (the measured FF is not available at this axial location) but are larger than the measured values at all radial locations.

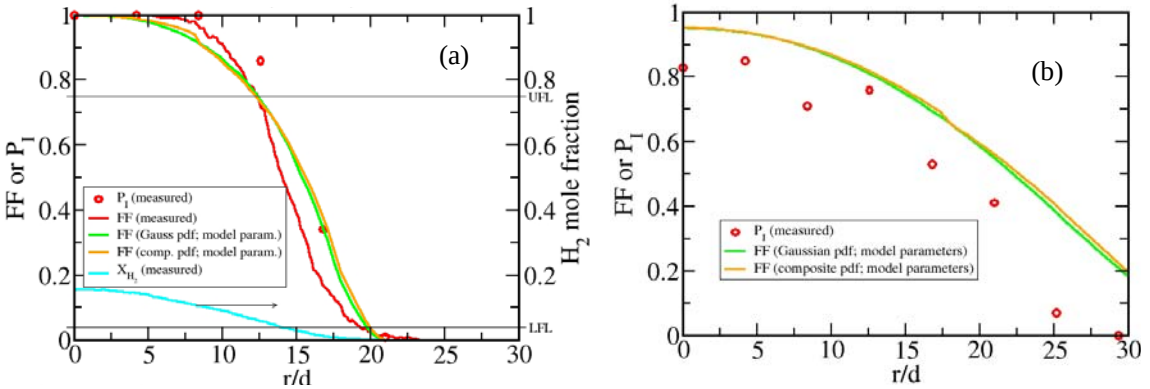

Figure 9. Predicted and measured FFs and measured P_Is along radial lines of vertical H_2 jet into air (Re=2384; Fr=268; d=1.91 mm): (a) z/d=89; (b) z/d=220; also shown in (a) are measured average X_{H2} and LFL and UFL values.

This trend continues at larger axial distances from the jet exit (not shown). The composite PDFs in Figs. 9a,b were evaluated using K=0.25 in (5); the resulting FFs are in very good agreement with FF determined using the Gaussian PDF at both axial locations (note that $\gamma \approx 1$ for r/d<20 at z/d=220). Similar agreement between predicted and measured FFs and P_Is was obtained for radial profiles in the CH_4 jet (not shown). Sensitivity of the predicted radial FF profiles to the constant K in (5) was noted for the CH_4 jet. Also shown in Fig. 9a are the measured radial profile of the average H_2 mole fraction and the static LFL and UFL values (0.04 and 0.75, respectively).

5.0 CONCLUSIONS

The ignition characteristics of turbulent H_2 jets into air have been studied. The probability of ignition (P_I) was determined using a pulsed Nd:YAG laser, focused to generate an ignition spark that served as the ignition source. A turbulent CH_4 jet was also studied to provide a baseline hydrocarbon fuel for comparison. Measurements in both CH_4 and H_2 jets exhibit similar trends in the ignition contours, which broaden radially in a linear fashion moving downstream until an axial location is reached where the contours move rapidly toward the centerline.

It was found that the time-averaged fuel concentration and conventional flammability limits established for quiescent fuel/air mixtures are insufficient to determine the flammable boundaries of the jets. Instead, integration of presumed probability density functions (PDFs) of local fuel concentration within the static flammability limits, termed the flammability factor (FF), was shown to provide a better representation of P_I for both H_2 and CH_4 jets. In addition to the ignition measurements, laser Rayleigh scattering experiments were used to characterize the fuel concentration throughout the jets.

Measurements of the H_2 concentration distribution at the time and location of the laser ignition spark are used to characterize the local composition statistics conditional on whether the laser spark results in a local ignition event or complete light-up of a stable jet flame. It was found that local ignition could only be obtained if the composition at the ignition point was within the static flammability limits.

Using measured values of the mean and fluctuating gas concentration, an empirically-based FF is obtained through direct integration of local PDFs. The FF was also determined using the mean and rms values of H_2 concentration obtained from computer simulations of the turbulent jet. Both Gaussian and two-part composite PDFs, where the PDF parameters, mean and rms fuel concentration, were evaluated from both measured data and model predictions and the intermittency factor was evaluated from a correlation, resulted in predicted FFs in good to excellent agreement with measured FFs, thus validating the approach for free jet flows of H_2. Comparisons were made along the jet centerline and along radial lines at several axial locations downstream of the jet exit for both H_2 and CH_4 jets. Both the functional forms of the assumed PDFs and the parameters used to evaluate the PDFs were validated by comparing with measured PDFs on and off the jet centerline and with measured centerline profiles of mean and rms quantities. A composite PDF that includes the effects of intermittency is required to predict the measured PDF in H_2 jets at large radial locations and for locations sufficiently far downstream of the jet exit. The radial profiles of the predicted FFs showed sensitivity to the value of a parameter in the intermittency correlation. Reduced empiricism in the predicted FF can be achieved by replacing the intermittency correlation with a transport equation in the model. Validation of a model for predicting FF (or P_I) in relatively simple turbulent jet flows has been carried out in this study. Extension of the model to more complex flows that occur when H_2 leaks are affected by walls, ground, and wind is a primary goal. Validated models can be used to provide a technical basis for the determination of safety distances in codes and standards regulations for flammable gases.

6.0 ACKNOWLEDGMENTS

This research was supported by the United States Department of Energy, Office of Energy Efficiency and Renewable Energy, Hydrogen, Fuel Cells and Infrastructure Technologies Program. Sandia is

operated by the Sandia Corporation, a Lockheed Martin Company, for the U.S. Department of Energy under contract DE-AC04-94-AL8500. Discussions with J.-Y. Chen, UC Berkeley, were helpful during the course of this work. This work was monitored by Antonio Ruiz.

7.0 REFERENCES

1. Swain, M., "Hydrogen Properties Testing and Verification", presented at Fuel Cell Summit Meeting, Coral Gables, Florida, June 17, 2004.
2. Swain, M. R., Filoso, P. A., and Swain, M. N., "An experimental investigation into the ignition of leaking hydrogen," *Int. J. Hydrogen Energy*, **32**, pp. 287-295, 2007.
3. Birch, A. D., Brown, D. R., Dodson, M. G., and Thomas, J. R., "The Turbulent Concentration Field of a Methane Jet," J. Fluid Mechanics, **88**, pt. 3, pp. 431-449, 1978.
4. Birch, A. D., Brown, D. R., Dodson, M. G., and Thomas, J. R., "Studies of Flammability in Turbulent Flows using Laser Raman Spectroscopy," 17th Int. Symposium on Combustion, The Combustion Institute, pp. 307-314, 1979.
5. Birch, A. D., Brown, D. R., and Dodson, M. G., "Ignition Probabilities in Turbulent Mixing Flows," *18th Int. Symposium on Combustion*, The Combustion Institute, pp. 1775-1780, 1981.
6. Pitts, W. M., "Effects of Global Density Ratio on the Centerline Mixing Behavior of Axisymmetric Turbulent Jets," Experiments in Fluids, **11**, pp. 125-134, 1991.
7. Schefer, R.W., Houf, W.G., Williams, T.C., "Investigation of Small-scale Unintended Releases of Hydrogen: Momentum-dominated Regime," Int. J. of Hydrogen Energy, **33**, pp. 6373-6384, 2008a.
8. Schefer, R.W., Houf, W.G., Williams, T.C., "Investigation of Small-scale Unintended Releases of Hydrogen: Buoyancy Effects," Int. J. of Hydrogen Energy, **33**, pp. 4702-4712, 2008b.
9. Smith, M. T. E., Birch, A. D., Brown, D. R., and Fairweather, M., "Studies of Ignition and Flame Propagation in Turbulent Jets of Natural Gas, Propane, and a Gas with a High Hydrogen Content," *21st Int. Symposium on Combustion*, The Combustion Institute, pp. 1403-1408, 1986.
10. Birch, A. D., Brown, D. R., Faireather, M. and Hargrave, G. K., "An Experimental Study of a Turbulent Natural Gas Jet in a Cross-Flow," Combust. Sci. Technol. **66**, pp. 217-232, 1989.
11. Kuo, K. K., Principles of Combustion, J. Wiley & Sons, New York, 1986.
12. Spalding, D. B., "Concentration Fluctuations in a Round Turbulent Free Jet," *Chemical Engineering Science*, **26**, pp. 95-107, 1971a.
13. Spalding, D. B., "Mixing and Chemical Reaction in Steady Confined Turbulent Flames," *13th Int. Symposium on Combustion*, The Combustion Institute, pp. 649-657, 1971b.
14. Schefer, R. W., and Dibble, R. W., "Mixture Fraction Field in a Turbulent Nonreacting Propane Jet," *AIAA Journal*, **39**, no. 1, pp. 64-72, 2001.
15. Bilger, R. W., Antonia, R. A., and Sreenivasan, K. R., "Determination of intermittency from the probability density function of a passive scalar," *The Physics of Fluids*, **v**. 19, no. 10, pp. 1471-1474, October, 1976.
16. Kent, J. H., and Bilger, R. W., "The Prediction of Turbulent Diffusion Flame Fields and Nitric Oxide Formation," *16th Int. Symposium on Combustion*, The Combustion Institute, pp. 1643-1656, 1977.
17. Cho, J. R., and Chung, M. K., "A k-ε-γ Equation Turbulence Model," *J. Fluid Mechanics*, **v**. 237, pp. 301-322, 1992.
18. Alvani, R. F., and Fairweather, M., "Prediction of the Ignition Characteristics of Flammable Jets Using Intermittency-Based Turbulence Models and a Prescribed pdf Approach," Computers and Chemical Engineering, **32**, pp. 371-381, 2008.
19. Chen, J.-Y., "Second-Order Conditional Modeling of Turbulent Nonpremixed Flames with a Composite PDF," *Combustion and Flame*, **v**. 69, pp. 1-36, 1987.
20. Moen, C. D., Evans, G. H., Domino, S. P., and Burns, S. P., "A Multi-Mechanics Approach to Computational Heat Transfer," *Proceedings 2002 ASME Int. Mech. Eng. Congress and Exhibition*, New Orleans, IMECE2002-33098, Nov. 17-22, 2002.